# Muon Production in Hadron-Hadron Collisions*

K. J. Anderson, G. G. Henry, K. T. McDonald,† J. E. Pilcher,‡
and E. I. Rosenberg
Enrico Fermi Institute, University of Chicago
Chicago, Illinois 60637

and

J. G. Branson, G. H. Sanders, A. J. S. Smith, and J. J. Thaler
Joseph Henry Laboratories, Princeton University
Princeton, New Jersey 08540

## Abstract

We report measurements of μ-pair production by $\pi^+$ mesons and protons. The production of J mesons is contrasted with the production of less massive particles. The character of the μ-pair continuum spectrum is discussed and implications for direct lepton production are given. Results are presented on a search for J production together with sources for additional final state muons.

Our group is engaged in a series of Fermilab experiments to study the characteristics of μ-pairs produced in hadron-hadron collisions. The data I will discuss today involves μ-pair masses below 4 GeV. These data are of interest at this conference on the production of new particles for several reasons.

First, we have a strong signal for inclusive J production. Since our spectrometer has rather broad acceptance as a function of the Feynman-x and $P_T$ of the μ-pair, we can study the production characteristics of the J, in

comparison with other vector mesons. The comparison can be made for both incident pions and protons and in this way, we may learn something of the production mechanism for the J.

The lower mass vector mesons are themselves of interest. For the past two years, there has been considerable stimulation by the observation of single direct leptons produced in hadron-hadron collisions. These leptons could originate from the leptonic or semileptonic decays of some yet unobserved particles. On the other hand, they might be one of a pair of muons which arises from vector meson decay or from a possible continuum component of the μ-pair mass spectrum. Since our experiment studies inclusive μ-pair production, including the vector mesons, down to masses of a few hundred MeV, we are in a position to settle this question. While the analysis of this phase of our experiment is still in progress, we can quote an upper limit on the cross section for the production of single muons which originate from a pair.

Lastly, it is interesting to look for final states containing 3 or more muons. Some theorists would have us believe that J's are produced together with charmed mesons.[1] While there are also counter arguments to this point of view,[2] it is a question that can be settled by any experiment with good acceptance for the muons which could arise from the semi-leptonic decays of the charmed particles. I shall present results on this study.

The detector used for this experiment was the Chicago cyclotron spectrometer, located in Fermilab's Muon Laboratory. The spectrometer, in its original form, was constructed by the Chicago-Harvard-Illinois-Oxford muon scattering collaboration and we are much indebted to this group for its use.

For the data I will discuss today, a 150 GeV/c unseparated positive beam of about $5 \times 10^5$/burst was incident on a 10-cm-thick beryllium target. Two helium filled beam Cerenkov counters, set just below the proton threshold, separated mesons from protons.

The detector is shown in Fig. 1. A 2.2-meter-thick iron shield, placed 1.3 meters downstream of the target, absorbed hadrons before they had an appreciable chance to decay. Particles leaving the shield passed through eight 1-meter-square MWPC planes and then into the cylindrical spectrometer magnet of 4.2 m pole diameter and 1.27 m gap height. Downstream from the magnet, trajectories were measured by 20 planes of wire spark chambers of size 2m × 4m or 2m × 6m. Particles were required to traverse an additional 2.5 m of steel to be detected in the triggering hodoscope labeled P in Fig. 1. For part of the running, four MWPC planes were placed just upstream of the hadron shield and four more were put halfway through the shield. These detectors allowed us to eliminate multiple scattering errors from the effective mass measurement and to reliably associate the observed pair with a primary interaction in the target. This is particularly important for μ-pairs of low mass and low $x_F$ where secondary production in the shield might otherwise pose a serious background.

The event trigger required exactly one unaccompanied particle in the beam, as determined by halo-veto counters around the beam, and by a pulse height restriction on one of the beam defining scintillators. At least two particles were required to leave the target by imposing a pulse height requirement on a counter located downstream of the target. The only other trigger condition of any consequence was the requirement that two non-adjacent counters be struck in the P-hodoscope.

The data analysis proceeded in a two-step process. First, the muon tracks seen in the spectrometer were reconstructed. Events were retained if they were consistent with the hypothesis that they originated in the beryllium target. The second step was to link the muon tracks of these events with data in the upstream MWPC planes. Figure 2 shows the μ-pair mass spectrum after the first step of the analysis. This sample is statistically more powerful than the one with the full analysis because the upstream detectors were only available for part of the run. The sample is free from shield associated background for μ-pair masses above 1 GeV. Note that the background from π and K decay, as monitored by the $\mu^+\mu^+$ and $\mu^-\mu^-$ events, is never more than about 15% of the non-decay background.

Figure 3 shows the mass spectrum below 1.4 GeV when the upstream MWPC's are used in the analysis. The data shown in this plot are corrected for reconstruction efficiency as well as the efficiency in triggering the detector. The latter is determined by normal Monte Carlo methods. The reconstruction efficiency is evaluated by superimposing Monte Carlo generated μ-pairs on the upstream MWPC data of real events and then trying to reconstruct the μ-pairs. In this way, the efficiency is mapped out as a function of the mass, $x_F$, and $P_T$ of the μ-pair. For example, the efficiency at $x_F = 0.2$ is constant for μ-pair masses greater than 500 MeV and falls to 50% of its plateau value at a mass of 240 MeV. The kinematic minimum for the μ-pair mass is, of course, $2m_\mu = 211$ MeV.

Signals from ρ-ω and φ decay to $\mu^+\mu^-$ are clearly seen in Fig. 3. The line widths are consistent with the uncertainty in the position of the interaction point along the length of the target. The continuum spectrum below

600 MeV may be partially due to background processes and this correction is still being evaluated. Nevertheless, cross sections for resonance production can be quoted and an upper limit placed on the cross section in the continuum. Figure 4 shows the line shape for J production, using the full data sample of the step one analysis.

The μ-pair production cross sections can be studied as a function of $x_F$ and $P_T$ for different mass regions. Figure 5 shows $Ed\sigma/dx$ for four different mass intervals integrated over $P_T$. The first two intervals are dominated by ρ-ω and φ production respectively. The absolute normalization in Fig. 5 corresponds to all events in the mass region, but the cross sections for the vector mesons and the continuum are given separately in Table I, together with fits of the form $Ed^3\sigma/d^3p = a(1-x_F)^c \exp(-bP_T)$. We have performed subtractions of the continuum component in the first two mass intervals and find that the fitted shapes for the $x_F$ and $P_T$ dependence of the remaining resonance signal are the same as without the subtraction. The $P_T$ spectra integrated over $x_F$ are given in Fig. 6. The width of the ρ-ω mass peak is slightly narrower than we would expect from ρ production alone, thus suggesting the presence of ω production. We make no attempt at this time to separate the contributions from ρ and ω production. For comparison with bubble chamber measurements of ρ production, we assume below that $\sigma_\rho = \sigma_\omega$.

We note that $Ed\sigma/dx$ for pion production of vector mesons is flatter than for proton production in all mass ranges. We find that at $x_F = 0.5$ pions are at least 4 times more likely to produce a J than protons. The corresponding figure for ρ production is less than a factor of 2.

We find that the exponential slope of the $P_T$ spectrum decreases with increasing μ-pair mass. This is true for both the resonances and the continuum. Figure 7 shows the b parameter as a function of μ-pair mass. The mean transverse momentum for J production is approximately 1 GeV/c.

In Table I we also present integrated production cross sections for $x_F > 0.15$, which is the region in which we have good detection efficiency, and for $x_F > 0$, which requires an extrapolation. The errors on the latter numbers reflect, in part, our uncertainty in the extrapolation. The cross sections per nucleon are obtained by using an $A^{2/3}$ dependence for mass intervals I and II, $A^{0.85}$ for mass interval III, and A for the J production. These are consistent with recent measurements of A dependence effects.[8]

Turning next to the question of the continuum component of the mass spectrum, we must consider first what contributions must exist from known sources. Any particle decaying to a final state containing a photon also has a decay mode in which the photon is replaced by a Dalitz pair. If sufficient energy is available, the Dalitz pair can be either an e-pair or a μ-pair. For example

$$\frac{\Gamma(\eta \to \mu^+\mu^-\gamma)}{\Gamma(\eta \to \gamma\gamma)} = 7 \times 10^{-4} \quad \text{and} \quad \frac{\Gamma(\omega \to \pi^0\mu^+\mu^-)}{\Gamma(\omega \to \pi^0\gamma)} = 7.3 \times 10^{-4}$$

according to calculations by Jarlskog *et al.*[3] and by Lai *et al.*[4] respectively. These Dalitz decay modes are much more serious if one is observing electrons instead of muons. In the case of η-decay the authors of Ref. 4 calculate that $\Gamma(\eta \to e^+e^-\gamma)/\Gamma(\eta \to \mu^+\mu^-\gamma) \simeq 23$.

These Dalitz decays contribute to the legitimate signal for inclusive μ-pair production. A source of background which must be subtracted, however,

is the photo-production of μ-pairs in the target. We have not yet finished evaluating this contribution and, therefore, we only quote an upper on the continuum signal.

The continuum components described above all have the common feature that the μ-pair carries only a fraction of the parent particle's energy. Thus, the $x_F$ and $P_T$ spectra should be steeper for these components. This effect is definitely seen for μ-pair masses below 500 MeV. A second feature of these sources is that they should be virtually absent for μ-pair masses above 1 GeV. We estimate that the Bethe-Heitler contribution is negligible above 1 GeV and in this mass range we know of no significant source of Dalitz μ-pairs. Figure 2 again shows the mass spectrum of the pairs and we note an apparent change in slope at 1.5 GeV. This shoulder could be the ρ'(1600) which is believed to have a width of several hundred MeV.[5] If the shoulder is interpreted as the ρ', the corresponding branching ratio to μ-pairs, times production cross section is 2 nb/nucleon for both proton and pion production. This should be considered an upper limit on ρ'(1600) production and decay to μ-pairs.

From the measurements described above, we can calculate an upper limit on the total cross section for inclusive μ-pair production by 150 GeV protons on nucleons. Using the A dependence already described and integrating over $M_{\mu\mu}$, $x_F$, and $P_T$, we obtain $\sigma_{\mu\mu} = 6.1$ μb/nucleon. Thus for the production of single muons from pairs $\sigma_\mu = 2 \times \sigma_{\mu\mu} = 12.2$ μb/nucleon. We calculate an upper limit on the $\mu/\pi$ ratio as $3.6 \times 10^{-5}$. There are several important points to bear in mind about this result. First, it cannot be compared directly with any existing prompt muon experiment because it is an average over all of phase space rather than being valid for any particular $x_F$ and $P_T$. The ratio is

dominated by the low $x_F$, low $P_T$, low mass region where the cross sections are the largest. Secondly, the ratio given is still an upper limit and may be reduced if backgrounds are found at low mass. In the near future, we will complete the evaluation of the background and then quote the result as a function of $x_F$ and $P_T$.

Finally, I would like to comment on our results for final states with more than two muons. In a sample of $1.0 \times 10^5$ $\mu$-pairs, we observe 164 events with 3 muons and 1 event with 4 muons. The mass spectrum for the $\mu^+\mu^-$ pairs of the 3 muon events is shown in Fig. 8. The $\mu^+\mu^-$ combination which gives the best vertex is used in the plot. The most obvious source of the extra muon is hadron decay. We estimate the decay probability times detector acceptance by using the like sign $\mu$-pairs whose rate is entirely consistent with that expected for hadron decay. On this basis, if we assume correlations are negligible, we expect one event in 800 to be accompanied by a hadron decay muon. Thus, we expect 125 3-$\mu$ events while we see 164. Since we have a sample of 130 J's, we expect about 0.2 J events to have extra muon from hadron decay. We see one event. Since the probability of seeing one event, when the expected number is 0.2, is 16% we conclude that we have no strong evidence that J's are accompanied by extra muons. A more quantitate statement depends on the details of the model being tested, and we forego this calculation until more data are available. We note that we have just finished a data taking run with a factor of 20 higher statistics. These data should pose a fairly stringent limit on the production of J's together with sources of extra muons.

In conclusion, we have seen interesting differences in the production of J-mesons by pions and protons, when compared with lower mass vector mesons.

The pion/proton cross-section ratio as a function of Feynman-x is significantly larger for J production than for the less massive vector mesons. The pion/proton asymmetry leads to a total cross section for J production by pions into the forward hemisphere which is approximately a factor of 2 larger than for protons. In the context of the parton model, where the J is produced from $c\bar{c}$ quarks in the sea, this result is surprising since the sea distributions are not expected to be substantially different for the various hadrons.[6]

The μ-pair measurements give a $\mu/\pi$ ratio, when integrated over all $x_F$ and $P_T$, which is somewhat less than the usually assumed value of $10^{-4}$. The results from this experiment do not appear inconsistent with measurements by Adair *et al.*[7] but at the present time, no direct comparison is made in the same kinematic region.

In a sample of 130 J events, we see only one case of a third muon and conclude that we have no clear evidence that J's are produced with particles which decay semileptonically.

## References


1. D. I. Sivers, Nucl. Phys. B106, 95 (1976).
2. See, for example, the paper by Halzen at this conference.
3. C. Jarlskog and H. Pilkuhn, Nucl. Phys. B1, 264 (1967).
4. Lai and Quigg, private communication.
5. For a recent review of available data on $\rho'$ production, see A. Silverman, Proceedings of the 1975 International Symposium on Lepton and Photon Interactions at High Energies (Stanford University, 1975).
6. An interesting proposal in this direction, based on the pion-proton differences for J production has been given by A. Donnachie and P. V. Landshoff, CERN preprint TH2166 (1976).
7. L. B. Leipuner *et al.*, Phys. Rev. Lett. 35, 1613 (1975), and H. Kasha *et al.*, Phys. Rev. Lett. 36, 1007 (1976).
8. M. Binkley *et al.*, Dimuon Production in Nuclear Targets, Columbia University preprint (to be published).



* This research was supported by the National Science Foundation and by the Energy Research and Development Administration.


† Enrico Fermi Postdoctoral Fellow.

‡ Alfred P. Sloan Fellow.

## Figure Captions

1. Layout of the detector.
2. Mass spectrum for all observed μ-pairs, without upstream analysis.
3. Mass spectrum below $M_{\mu\mu}$ = 1.4 GeV with upstream analysis. Pion-induced and proton-induced events are combined in this plot.
4. Line shape of the J signal.
5. Dependence of μ-pair production on Feynman-x of the pair in various mass intervals. The lines indicate best fits to the data using the parameterization $Ed\sigma/dx = A(1-x_F)^C$. The data are integrated over $P_T$.
6. Dependence of μ-pair production on transverse momentum of the pair, for various mass intervals. The lines indicate best fits to the data using the parameterization $d\sigma/(P_T dP_T) = B\exp(-bP_T)$. Data are integrated over Feynman-x.
7. The dependence of b, the slope in $P_T$, on the μ-pair mass.
8. The mass spectrum of $\mu^+\mu^-$ pairs for events where three muons are observed.

## Table Caption

Table I Results of fitting the Lorentz invariant cross section to the form $Ed^3\sigma/d^3p = a(1-x_F)^c \exp(-bP_T)$ for different regions.

Table I

| Region | Mass $GeV/c^2$ | Source | a $nb/GeV^2/c^3$ | b $(GeV/c)^{-1}$ | c | Cross Section per Nucleus $x_F > 0.15$ nb | Cross Section/Nucleon $x_F > 0.15$ nb | $x_F > 0$ nb |
|---|---|---|---|---|---|---|---|---|
| | | | Proton Production | | | | | |
| I | 0.65 - 0.93 | ρ-ω | $3.51 \pm .5 \times 10^3$ | 3.83±.09 | 2.34±.12 | 824±165 | 190±40 | 520±170 |
| | | Continuum | $1.37 \pm .4 \times 10^3$ | | | 323±65 | 75±15 | 210±70 |
| II | 0.93 - 1.13 | φ | 697±140 | 3.90±.27 | 3.43±.36 | 104±20 | 24±5 | 74±25 |
| | | Continuum | 353±110 | | | 52±10 | 12±2.4 | 37±12 |
| III | 1.13 - 2.10 | Continuum | 127±38 | 3.26±.80 | 2.95±.80 | 28.4±6 | 4.4±.9 | 11±4 |
| IV | 2.7 - 3.5 | J | 36.±12 | 2.08±.26 | 2.94±.32 | 14.0±4 | 1.6±.5 | 3.4±1.1 |
| | | | Pion Production | | | | | |
| I | 0.65 - 0.93 | ρ-ω | $2.54 \pm .5 \times 10^3$ | 4.24±.16 | 1.09±.13 | 830±170 | 190±40 | 410±140 |
| | | Continuum | $1.09 \pm .3 \times 10^3$ | | | 354±70 | 82±16 | 180±60 |
| II | 0.93 - 1.13 | φ | 340±85 | 3.64±.40 | 1.21±.40 | 136± 30 | 31±6 | 63±20 |
| | | Continuum | 101±30 | | | 41±8 | 9.5±2 | 19±6 |
| III | 1.13 - 2.0 | Continuum | 61.8±20 | 3.32±.73 | 0.98±.52 | 31±6 | 4.7±1 | 8.3±2.8 |
| IV | 2.7 - 3.5 | J | 80±27 | 2.57±.36 | 1.72±.20 | 34±10 | 3.8±1.1 | 6.7±2.2 |

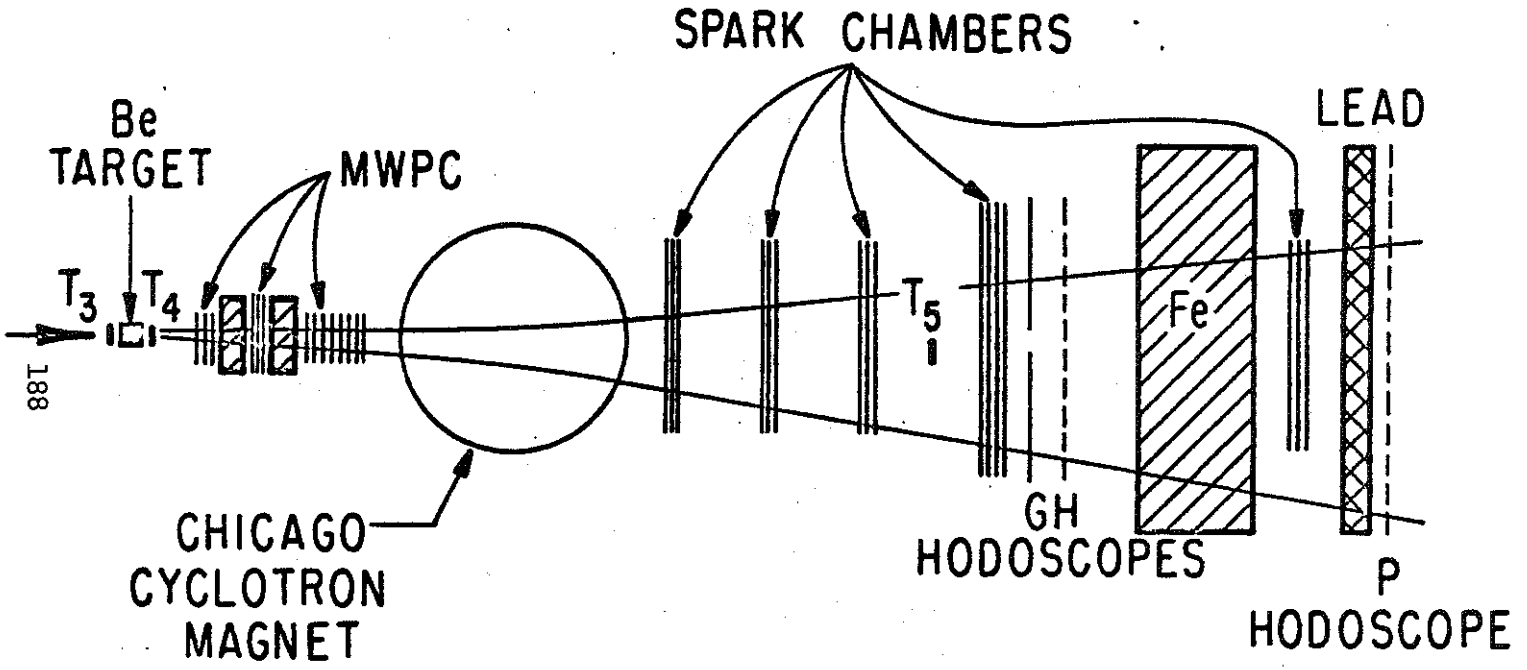
SPARK CHAMBERS
LEAD
Be
TARGET
MWPC
T3
T4
T5
Fe
188
CHICAGO
CYCLOTRON
MAGNET
GH
HODOSCOPES
P
HODOSCOPE

FIGURE 1

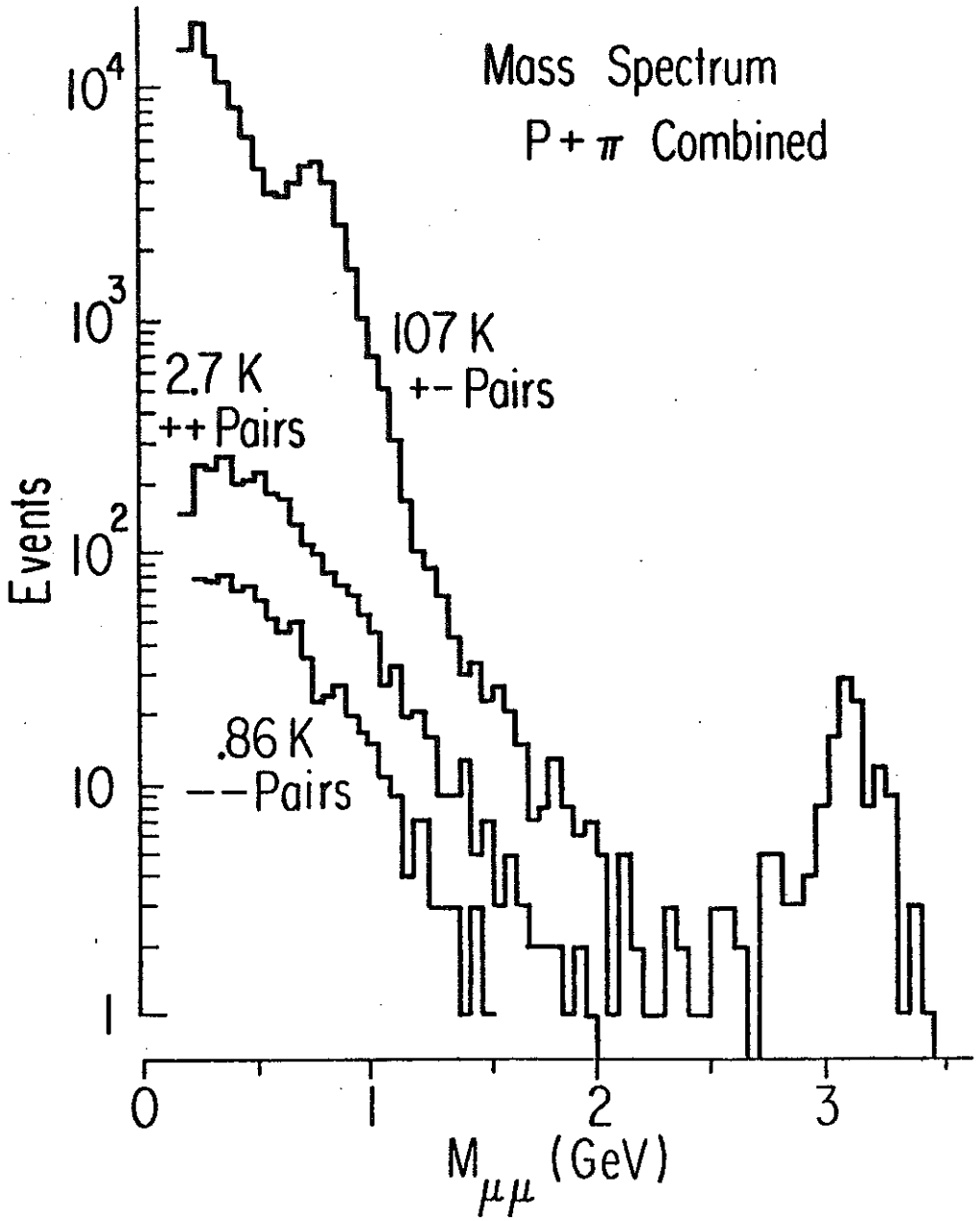
Mass Spectrum
P + π Combined
10^4
10^3
10^2
10
1
Events
107 K
+- Pairs
2.7 K
++ Pairs
.86 K
-- Pairs
0
1
2
3
M_μμ (GeV)

FIGURE 2

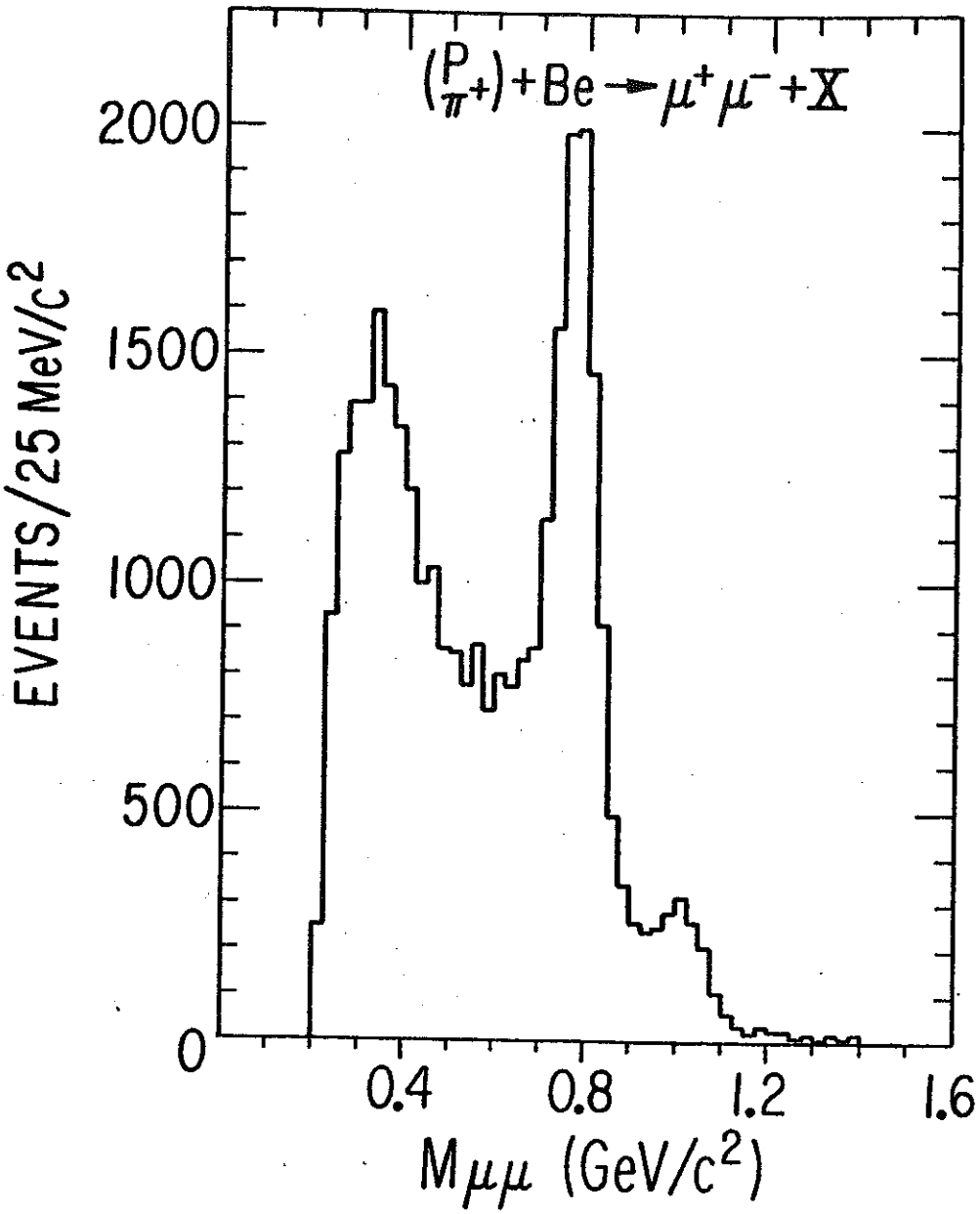
$(P_{\pi^+}) + Be \rightarrow \mu^+\mu^- + X$
EVENTS/25 MeV/c$^2$
2000
1500
1000
500
0
0.4
0.8
1.2
1.6
$M\mu\mu$ (GeV/c$^2$)

FIGURE 3

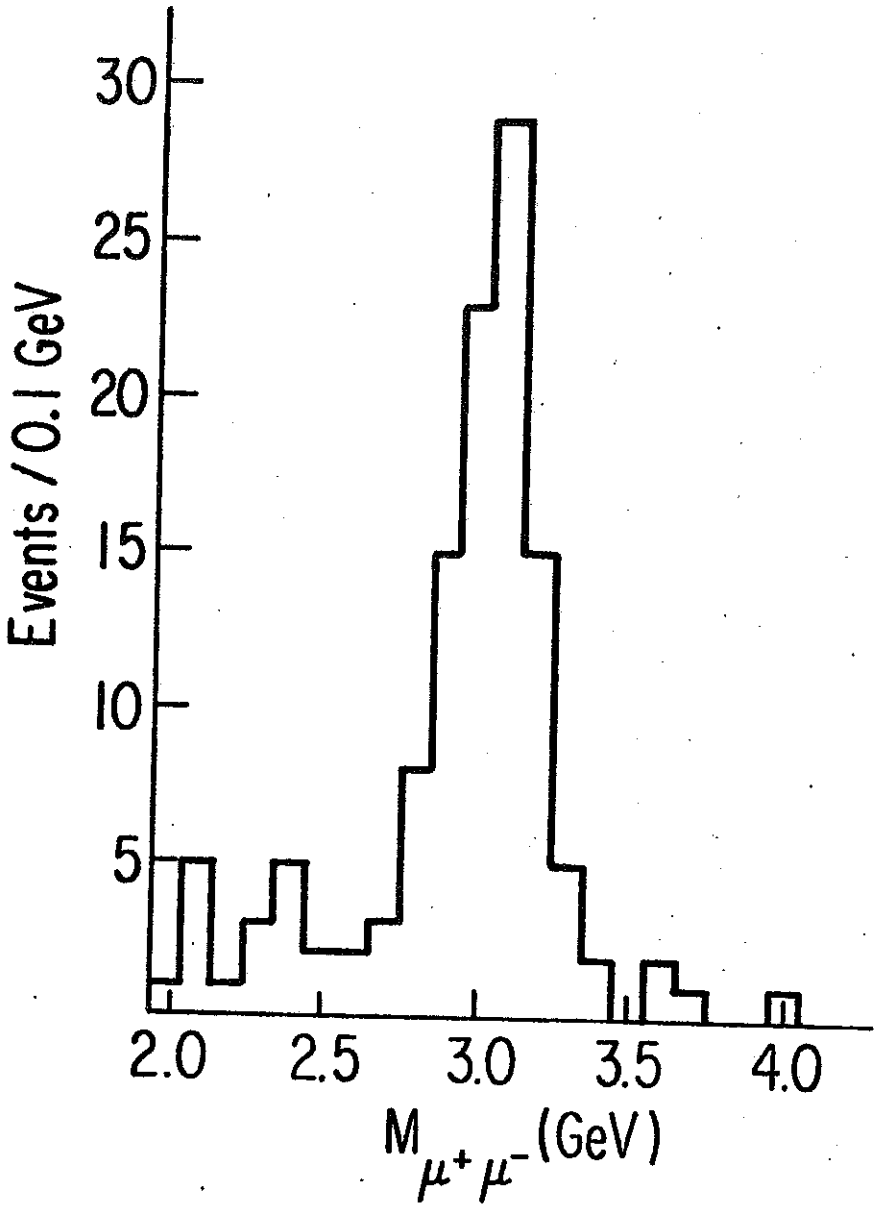


FIGURE 4

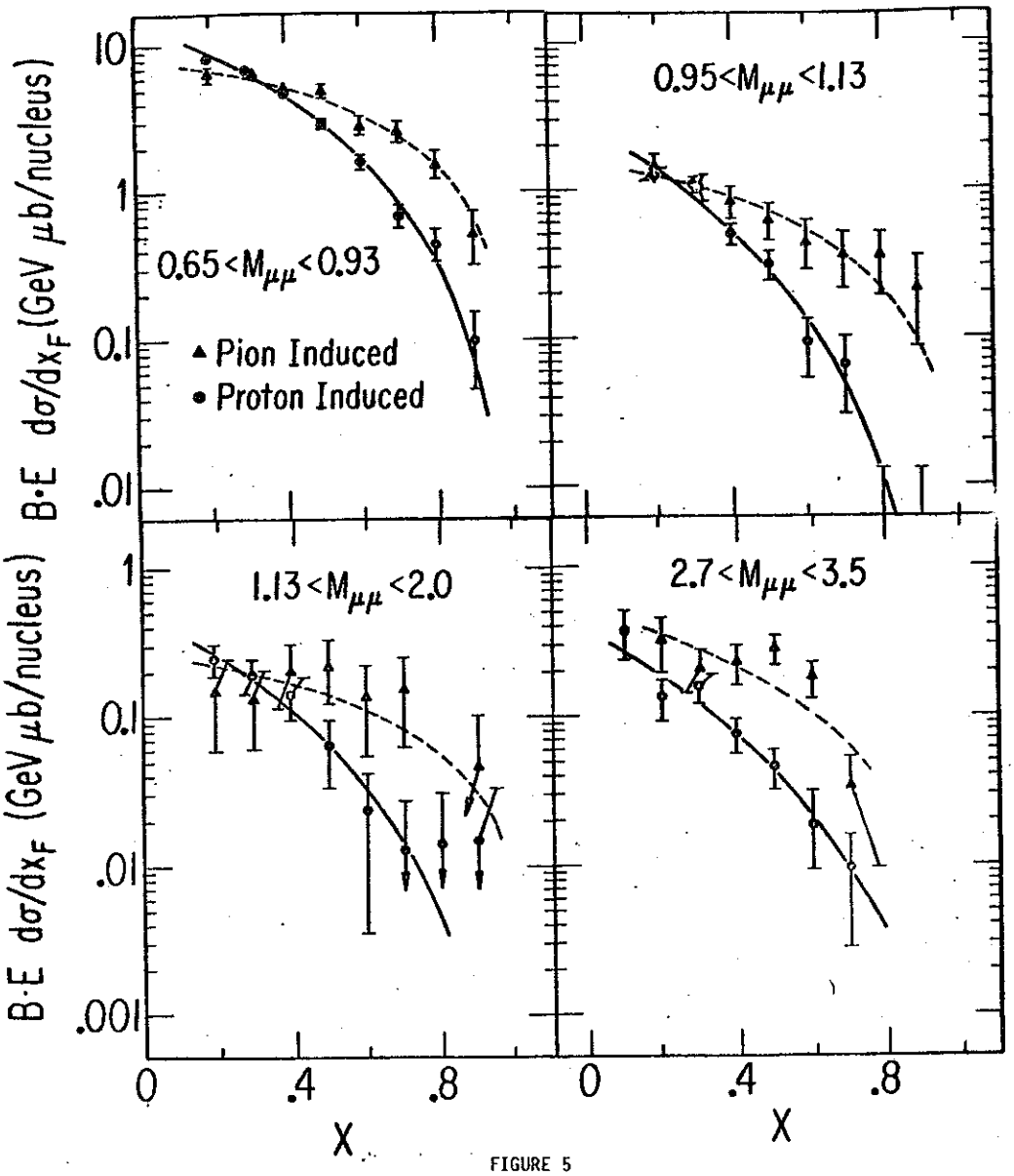
B·E dσ/dx_F (GeV μb/nucleus)
10
1
0.1
.01
0.65<M_μμ<0.93
▲ Pion Induced
• Proton Induced
0.95<M_μμ<1.13
1.13<M_μμ<2.0
2.7<M_μμ<3.5
1
0.1
.01
.001
0
.4
.8
X
0
.4
.8
X

FIGURE 5

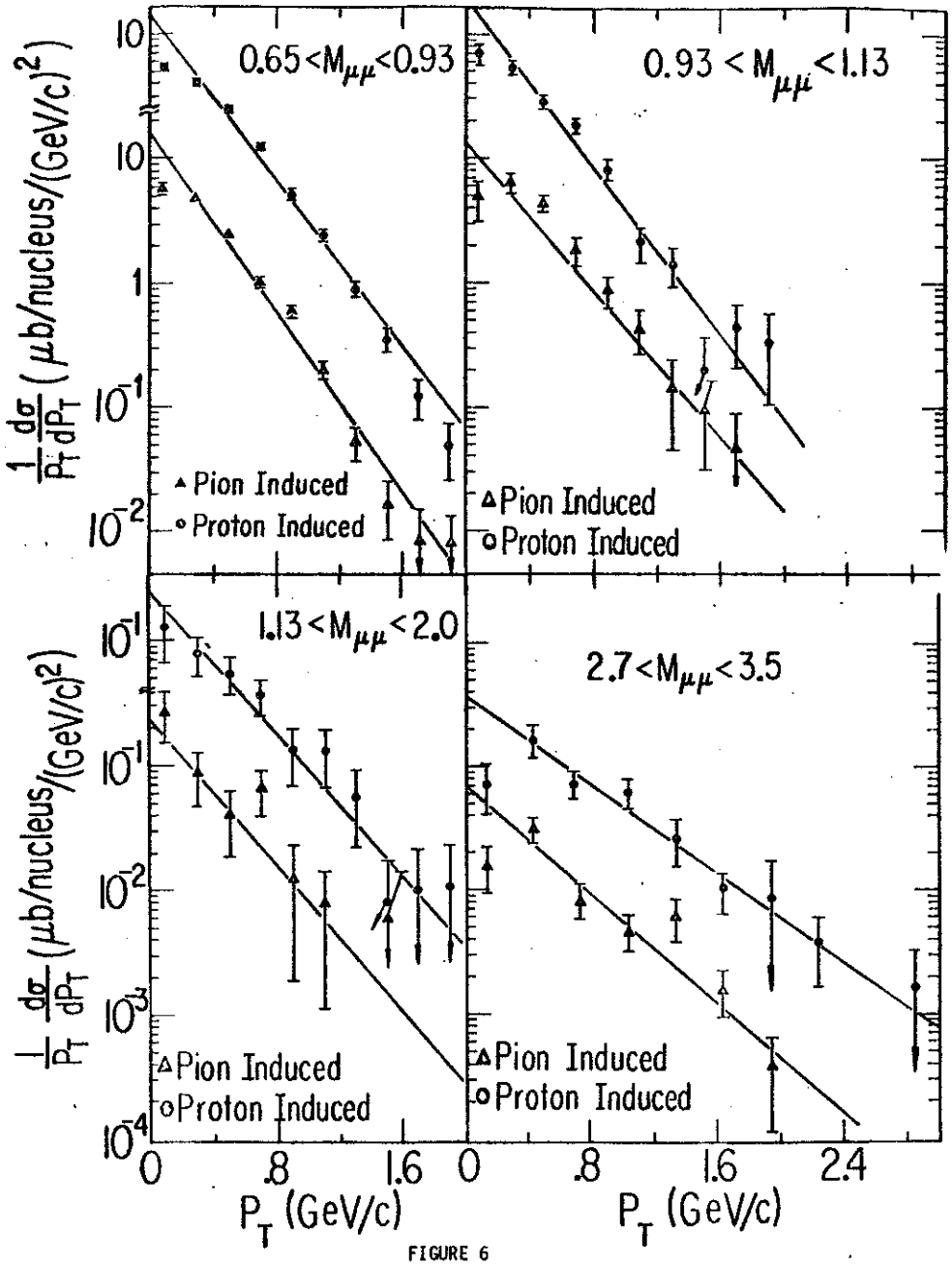
0.65<Mμμ<0.93
0.93 < Mμμ<1.13
1.13<Mμμ<2.0
2.7<Mμμ<3.5
Pion Induced
Proton Induced
1/PT dσ/dPT (μb/nucleus/(GeV/c)²)
PT (GeV/c)

FIGURE 6

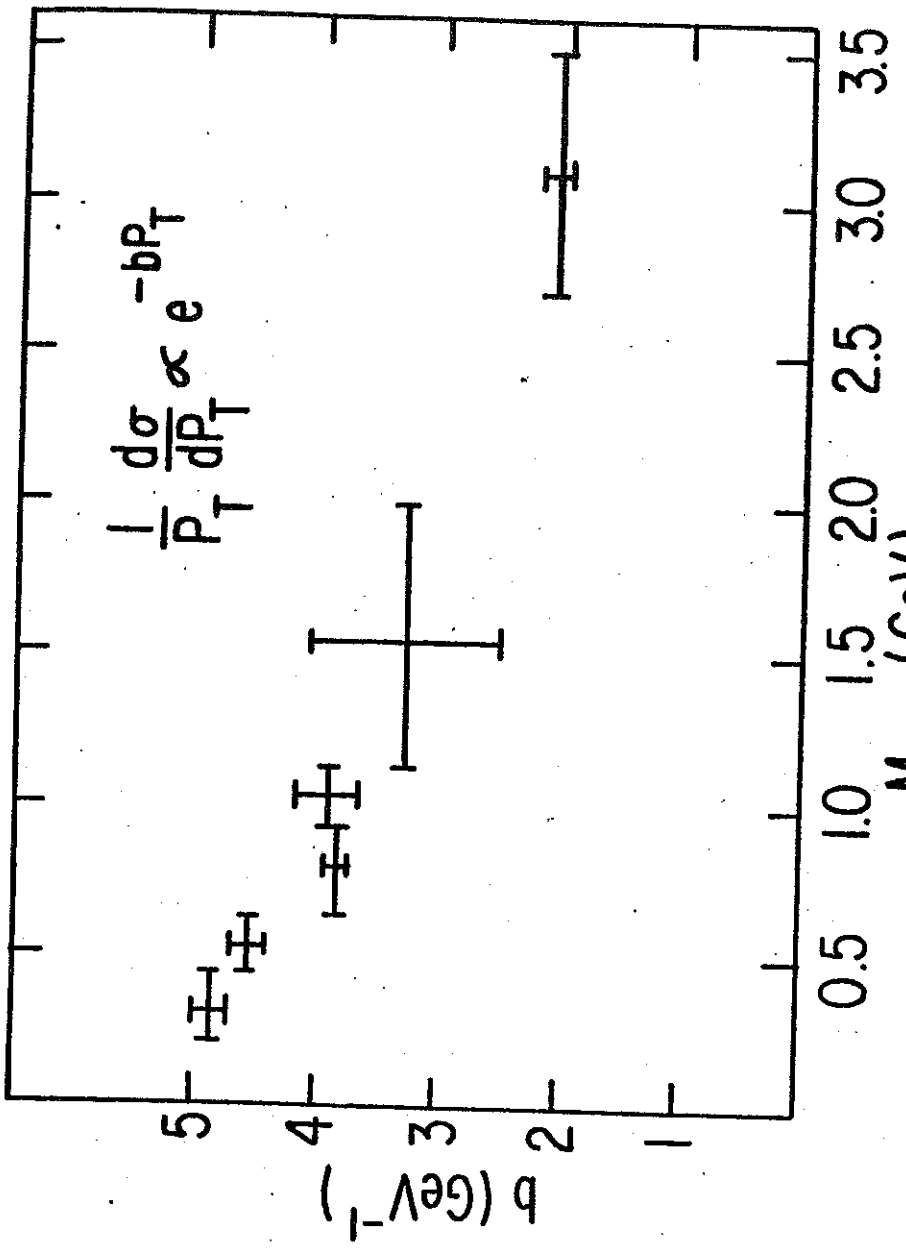
$\frac{1}{P_T}\frac{d\sigma}{dP_T} \propto e^{-bP_T}$
b (GeV$^{-1}$)
$M_{\mu\mu}$ (GeV)
0.5
1.0
1.5
2.0
2.5
3.0
3.5
1
2
3
4
5

FIGURE 7

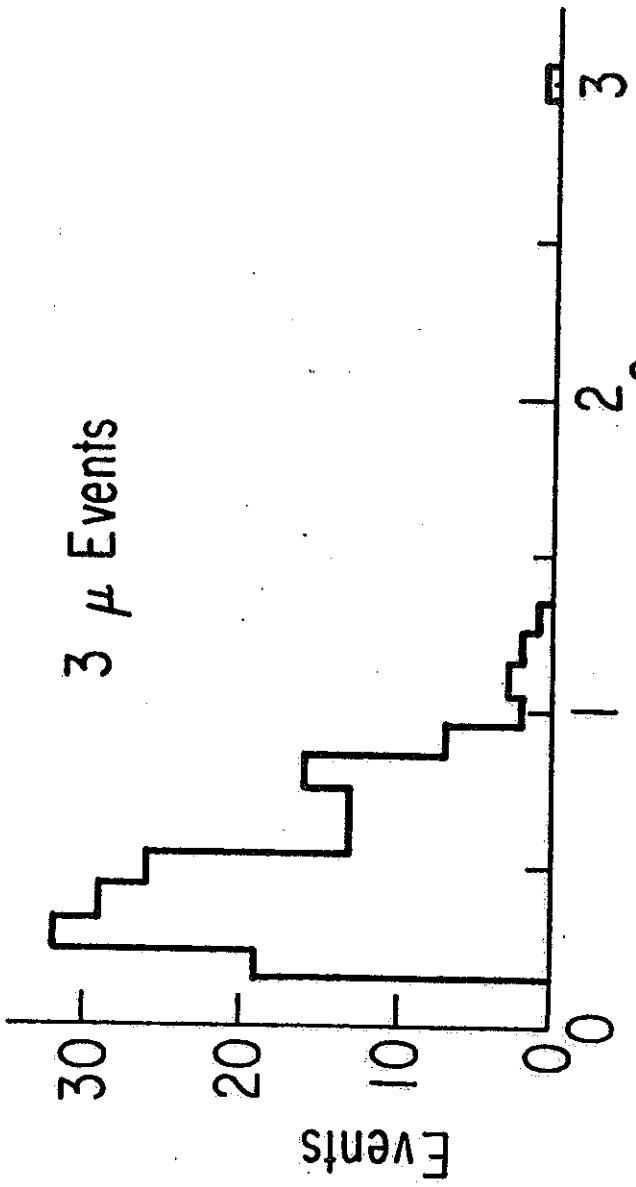


FIGURE 8